

A printable P(VDF-TrFE)-PZT Composite with Very High Piezoelectric Coefficient

Tuomo Siponkoski^{a*}, Mikko Nelo^a, Heli Jantunen^a, Jari Juuti^a

^aMicroelectronics Research Unit, P.O. Box 4500, 90014, University of Oulu, Finland.

*Corresponding author: Tuomo Siponkoski, tuomo.siponkoski@oulu.fi

Co-authors: Dr. Mikko Nelo, mikko.nelo@oulu.fi, Prof. Heli Jantunen, heli.jantunen@oulu.fi

Dr. Jari Juuti, jajuu@ee.oulu.fi

KEYWORDS: Electrical properties; Mechanical properties; Piezoelectricity; Polymer-matrix composites (PMCs); Printed electronics (PE)

Abstract

In this paper a significant advance in the piezoelectric properties of poly(vinylidene fluoride-trifluoroethylene)-lead zirconate titanate (P(VDF-TrFE)-PZT) composite ink has been achieved by coating the ceramic particles prior to formulation with a polymeric surfactant containing carboxylic acid anhydride functional groups and the piezoelectric response of a unimorph cantilever is further enhanced by introducing a reinforced substrate. The measured effective transverse piezoelectric coefficient ($d_{31\text{eff}}$) was -56 pm/V, which is 3.3 times higher than that of the same composite without surfactant and is the highest reported for a printable polymer-ceramic composite. In addition, the printability of the ink and dispersion of the ceramic particles was enhanced. The samples were fabricated by stencil printing of a single piezoelectric layer on a flexible PET substrate followed by curing at only 120 °C, thus enabling utilization on a wide range of substrates. The results also show the improved particle dispersion and layer quality in 0-3 composite inks with surfactant added and the effect of sample structure and mechanical coupling between the hard ceramic particles and the soft

matrix. The developed composite ink is suitable, for example, in sensors in printed wearable and portable electronics.

1. Introduction

In modern electronics and the Internet of Things (IoT), there is an ever-growing interest in the further integration of electronic devices. In applications, for example in the fields of Body Area Networks (BAN) or Structural Health Monitoring (SHM), the demand for integration stems from the need for lightweight, flexible, wearable and large area electronic structures. Applications and components possessing these properties need to be realized with cost effective manufacturing processes. These requirements are the driving force for research into fabrication processes and materials in printed electronics. Basic printing techniques such as roll-to-roll, inkjet, flexography and gravure printing offer the usage of temperature sensitive, flexible and lightweight substrates (papers and polymers). The cost of the components or applications can be reduced with high-volume manufacturing, which is also one of the characteristic properties of printed electronics. [1–5]

An important area of applications in electronics covers sensors, actuators and energy harvesters. Due to their versatile properties, piezoelectric materials such as lead zirconate titanate, (PZT, $\text{Pb}(\text{Zr},\text{Ti})\text{O}_3$) are suitable for the active components in such applications. [6–10]. However, in order to combine the benefits of piezoelectric materials, printing technologies and low fabrication temperatures it is necessary to use materials which are solution processable and which can be modified to form printable inks. There are two main categories in the class of lightweight and low temperature (<300 °C) fabricated piezoelectric materials. The first is piezoelectric polymers such as poly(vinylidene fluoride) (PVDF) and its copolymers (e.g. with trifluoroethylene, TrFE),

and the second is organic-inorganic composites, where the filler and/or the matrix materials are piezoelectric. Piezoelectric polymers have been studied for some decades and are available from several manufacturers. In addition, their usage in printable composites research has increased during the last few years, but these materials are still not fully utilized in printed electronics. [11–20]

In the present study, copolymer P(VDF-TrFE) 56/44 mol.% was selected as the matrix material in the developed composite because the polymer chains in it conforms to the ferroelectric and piezoelectric β phase (as in PVDF), and it also has the highest relative permittivity in this polymer family. A higher permittivity is beneficial in poling due to the improved electric field coupling with the very high permittivity ceramic particles. [11,12] It is also commonly known that PVDF and its copolymers have piezoelectric coefficients of opposite signs, as compared to ceramic piezoelectrics, because of the origin of the piezoelectricity. [19] This reduces the effective coefficients in ceramic-polymer composites of these two materials. The selected 56/44 mol.% copolymer also has smaller piezoelectric coefficients and coupling coefficients than those of other VDF-rich copolymers [11]. This maximizes the net piezoelectric coefficient of the composite when both phases are poled in the same direction. The poling in this work was done in the same direction for both of the materials in order to enable the comparison of the new composite ink with previous versions and to keep the sample conditioning simple at this stage of the research.

In addition, when making inorganic-organic composites, especially composite inks, two very important issues arises: the dispersion of the filler particles and the interface mismatch between the matrix and the filler. In many cases, the surface of ceramic fillers interact poorly with the polymer matrix causing, for example, agglomeration, voids and degraded electrical properties. One way to minimize this is the activation of the surface

of the particles with surfactants or other treatments. [21–28] These treatments enhance the coupling between the filler particles and the matrix material, which leads to better distribution of the filler and higher break-down electric fields. Particularly in the case of piezoelectric composites, the mechanical coupling is very important in order to utilize the beneficial properties of the piezoelectric filler. [29] In the present study, a polymeric surfactant with carboxylic acid anhydride functional groups was used. The microstructure, dielectric, ferroelectric and electromechanical properties of the developed printable piezoelectric composite are reported, analyzed and a comparison is made with our earlier reported results [14] of a similar composite which had no surface treatment. The results of the newly developed composite show good potential for the material to be used in sensors or actuators. Moreover, the work is viewed as an important step towards the utilization of printing technologies in piezoelectric sensor fabrication in future electronics applications.

2. Materials and Methods

2.1. Ink formulation & sample printing

The ceramic particles used as a filler were PZ29 (Ferroperm Piezoceramics A/S & Meggitt, Denmark), with an average particle size of 1.3 μm (measured with a Beckman Coulter LS 13320 laser diffraction analyzer). Copolymer P(VDF-TrFE) 56/44 mol.% (Solvay-Solexis, Belgium), was used for the polymer matrix in the ink. Silver ink 5064H (DuPont, USA) was used as the electrode material. These materials were the same as those used in our previous research [14]. The chemical used to coat the ceramic particles was a polymeric surfactant MalialimTM AAB-0851 (NOF Co., Japan), with carboxylic acid anhydride functional groups in each repeating unit. It has been successfully used previously for ink with barium titanate particles in a shunt capacitor [15].

In the formulation of the composite ink, the required amount of surfactant for surface coating of the particles was first calculated on the basis of the specific surface area of the PZT particles ($4 \text{ m}^2/\text{g}$) and the surface area occupied by one repeating unit of the surfactant polymer (0.45 nm^2). Next, the surfactant was dissolved in acetone and 2-(2-Butoxyethoxy) ethyl acetate (>99.2%, Sigma-Aldrich, Germany) and the PZT particles were weighed and added. The mixture was then milled for 16 hours in a planetary ball mill. The amount of surfactant was thus minimized and the milling effectively broke up any possible agglomerations in the PZT powder. The copolymer was dissolved with dimethylformamide (>99%, Fluka) and the correct amount of this solution to form 48 vol.% filler content was added to the surfactant-treated PZT particles and mixed in a ball mill for 16 hours. The volume percentage of filler particles was selected to be slightly below 50 vol.% because this had been found from earlier investigations to result in high quality printed samples [14]. After mixing, a suitable viscosity for screen printing was attained by evaporating excess solvent. A typical ink batch consisted of about 30 grams of ceramic particles and about 36 grams of dissolved copolymer (20 wt.%). For each sample, a single layer of composite was printed with a $200 \mu\text{m}$ thick steel stencil on a $100 \mu\text{m}$ thick PET polymer substrate. The maximum temperature used in curing the composite layer and the electrodes was $120 \text{ }^\circ\text{C}$. Additionally to increase the resonance frequency of the cantilever samples in converse piezoelectric measurements, some samples were reinforced by gluing a $50 \mu\text{m}$ steel foil to the bottom of the PET using a cyanoacrylate adhesive. (Sample structures; Fig. S1, Supplementary Material)

2.2. Mechanical properties and microstructure

The adhesion of the cured composite layer to the silver electrode was tested with a pull-off strength tester, Positest AT-A (DeFelsko, USA) and a tape peel-test using a 107 X-Hatch kit (Elcometer, UK). In the pull-off test, the samples were fixed to a rigid surface

and Ø 20 mm aluminum dollies were glued to the composite layer. The pull-off strength was measured according to the ISO 4624 standard and the failing point of each sample was determined. In the tape-peel test, sample surfaces were cut with cross-cuts to form a lattice pattern, a standard (ISO 2409) adhesive tape (from Scapa Group) was glued on top of the pattern and then peeled off. The results were visually assessed and the number of damaged squares calculated.

The Young's modulus of the composite layer, substrate and steel foil was measured by using a tensile stress testing stage (TST350, Linkam, UK) using a strain rate of 1 % per minute. The modulus was calculated from the ratio of applied stress and strain of the sample in the tensile direction. The equations and material parameters used are provided in the Support Information.

The microstructure and layer thicknesses of the printed and cured composites were investigated from the cross-section of the composite samples by FESEM (Ultra Plus, Zeiss, Germany) and a polarized light microscope. The samples for SEM were cut with a laser (LPKF Proto Laser U3, LPKF Laser & Electronics AG, Germany) and cast in a mold epoxy. After curing, the cross-section on top of the mold samples was polished gently with sandpapers and diamond polishing suspension. The melting temperature and crystallization of the ink were investigated from 4.5 mm diameter laser cut samples on a PET substrate using DSC-TGA (J9 Jupiter, Netzsch, Germany) and compared with samples without surfactant on the filler particles [14].

2.3. Dielectric and electromechanical characterization

The dielectric properties were measured from 1 kHz to 1 MHz with a 1 Vpp signal amplitude using an LCR meter (HP 4284A, Keysight Technologies, USA). The ferroelectric properties, hysteresis loops and remanent polarization (P_r) were measured

at 2.5 Hz up to 28 MV/m electric field with a high voltage ferroelectric tester (LC Precision with 10kV HVI-SC, Radiant Technologies, USA). Samples were poled in a 15 MV/m electric field at room temperature for 1 hour and shorted after the poling process. The effective transverse piezoelectric coefficient $d_{31\text{eff}}$ was determined using the tip displacement from cantilever shaped samples in an AC field (Measurement setup; Fig. S2, Supplementary Material). Measurements were conducted using a Laser Doppler–vibrometer (OFV-552 measuring probe, Polytech GmbH, Germany) and a high voltage amplifier after a delay of at least 48 hours from poling. The total number of samples in the piezoelectric measurements was 7.

3. Results and Discussion

Backscattering FESEM images of cross sections of typical cured samples both with and without surfactant coating on the filler particles are shown in Fig. 1a and 1b, respectively. In the surfactant treated composite the cluster size was notably smaller (Fig. 1a) where only a few, if any, agglomerates were visible. In the composite without surfactant treated filler, there are several agglomerates visible (Fig. 1b). By limiting the formation of agglomerates, the filler particles were distributed more homogeneously in the composite matrix.

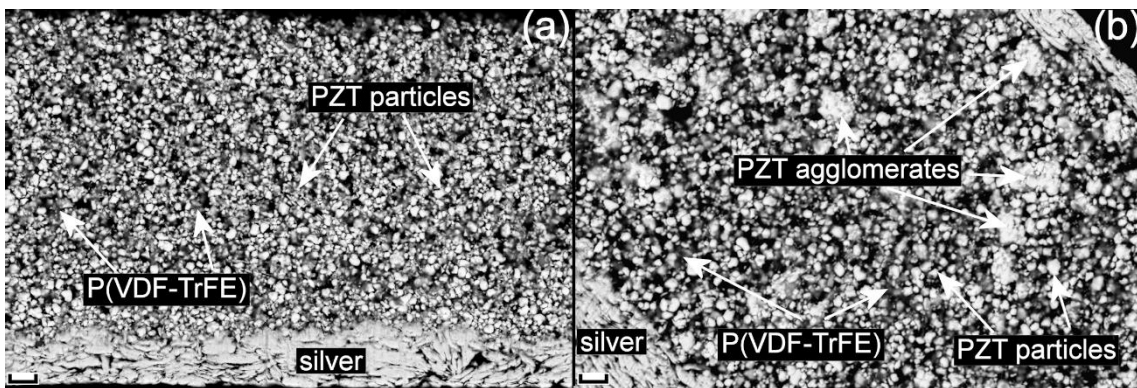


Fig.1. Backscattering FESEM images of cured samples with surfactant (a) and without surfactant (b). PZT particles, copolymer matrix and agglomerates are marked with white arrows. Scale bar = 3 μm .

Fig. 2 shows a typical test result from the cross-hatch tape peel test. Cured composite layers all showed ISO 2409 results between 0 and 1, meaning that the edges of the cuts were smooth and either none or a maximum of 5 % of the squares were affected at the intersections of the cuts. This showed that the ink had excellent adhesion to itself and did not peel off in the test. This result was similar to that of an earlier composite produced without a coating of filler particles [14]. Thus, the addition of the surfactant had no notable effect on the peel-off adhesion. In a pull-off strength test, the surfactant-modified composite gave $2.70 (\pm 0.16)$ MPa as an average result. A typical break point in this test was observed at the interface of the lower electrode and the cured composite layer, i.e. the strength of the composite was higher than the measured pull-off strength value in the test.

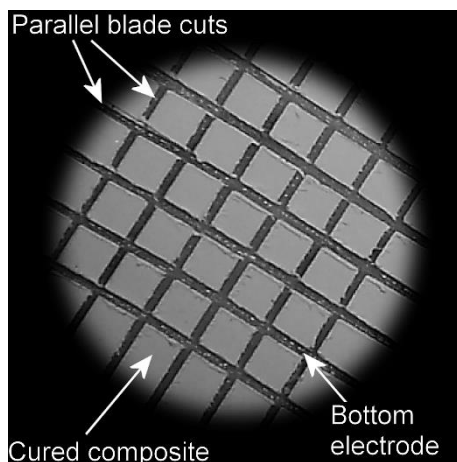


Fig. 2. A typical result of a cross-hatch tests on the composite (with surfactant) surface showing 0 result (ISO 2409) where all sample squares are intact.

Fig. 3 shows the Differential Scanning Calorimeter (DSC) data recorded from unpoled composites both with and without the surfactant treatment on the ceramic particles. The first endothermic peak was found at 63 °C and the second endothermic peak at 152 °C in both samples, which corresponded well with the phase transformation temperature of the copolymer from the ferroelectric β phase into the paraelectric phase and the melting point of the copolymer, respectively. [11, 12, 31–34]

The two DSC curves were very similar to each other, suggesting that addition of the surfactant had only a very small or zero effect on the characteristic temperature or the level of crystallinity of the polymer matrix. The broad maximum around 100 °C was due to the fact that the PET substrate was not completely compensated by the correction measurement derived from a pure PET substrate. Nevertheless, the effect was similar in both composite versions, thus indicating stable measurement conditions.

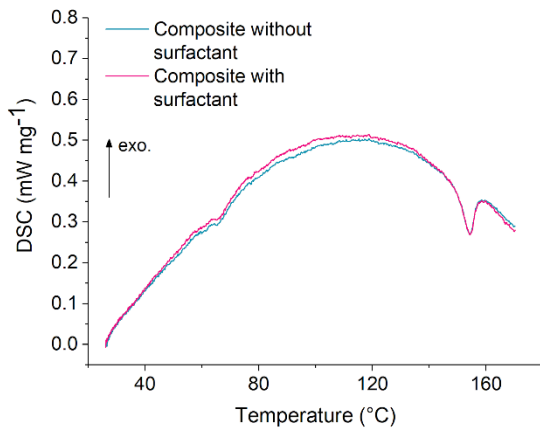


Fig. 3. DSC measurement showing heat flow of P(VDF-TrFE)-PZT composite on PET substrate with (blue) and without (red) surfactant.

Fig. 4 shows the dielectric properties of the composite samples at temperatures of 18–110 °C and frequencies from 21 Hz to 1 MHz (capacitances from about 4.5 nF to 3 nF, respectively). At 1 kHz the relative permittivity (ϵ_r) and loss tangent ($\tan\delta$) were 58 (std. dev. ± 5 % between samples) and 0.03 (std. dev. ± 6 % between samples), respectively. The relative permittivity decreased with increasing measurement frequency and the change became steeper at higher frequencies (Fig. 4a). The losses increased rapidly after 1 kHz until the limit of the measurement range and the maximum was seen just before 1 MHz. This was assumed to be related to relaxation in the β_1 -transition in the amorphous region in the copolymer rich in TrFE-units and it was shifted to higher frequencies when the temperature increased. The transition behavior and dielectric properties of the TrFE and VDF copolymers have been investigated by T. Yagi et al. who describe the behavior in more detail [12]. Compared to the earlier made composite with 50 vol.% of PZT without surfactant [14], the ϵ_r was about 18 % less and $\tan\delta$ at 1 kHz was 16 % less in the case of the composite with surfactant presented here. The decrease in permittivity was partly due to the smaller amount (50 vol.% vs. 48 vol.%) of ceramic particles in the composite (permittivity difference 8–10 % using the commonly used Bruggemans model [16, 18]). Also, the surfactant has a low permittivity whereas P(VDF-TrFE) is known to be a polymer with very high permittivity (Table 1), and about 2.5 vol.% of the P(VDF-TrFE) was replaced with surfactant in the present composition (compared to 48 vol.% composite without surface treatment) [12, 35]. These two effects are evident from the compositional differences between the two composites. Nevertheless, it could be expected that the increased dispersion of filler particles and smaller amount of porosity would increase the permittivity. Since there was no clear increase in permittivity and the quality of the cured layers and the distribution of particles (no agglomerates) has been verified, the

smaller effect of interface polarization could explain the overall decrease in dielectric properties. The fact that the surfactant also passivates the particles' surface supports the observation. Passivation limits the introduction of residual ions by the ceramic filler and limits the mobility of charge carriers in the matrix: these affect the permittivity of the composite. [36–39] The effect of interface polarization is considered further when the ferroelectric response of the composites is discussed. The decrease in losses can be understood via structural changes in the polymer chains introduced by the filler particles and a general enhancement in the cured layer quality associated with fewer agglomerations and pores. [38–42]

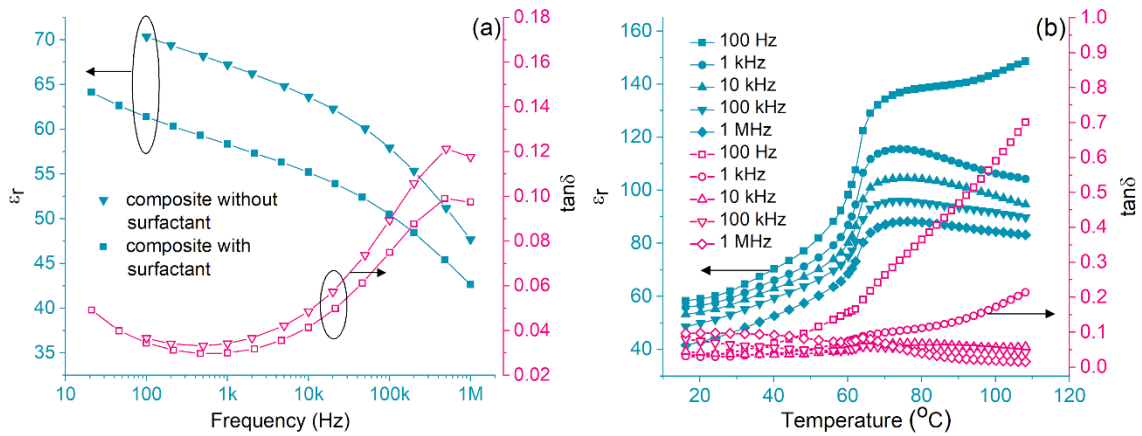


Fig. 4 Dielectric properties of composite with and without surfactant (previous study) measured from 100 Hz to 1 MHz (a) and for composite with surfactant at temperatures from 18 to 110 $^{\circ}\text{C}$ (b). Solid symbols are for relative permittivity and open symbols for loss tangent. Square symbols are for composite with surfactant (this study).

The temperature dependence of the dielectric properties of the newly developed composite with surfactant is shown in Fig. 4b. The curves exhibit a steep increase in permittivity between 65 to 73 $^{\circ}\text{C}$ showing about 50 % increase at all presented

frequencies. This is typical behavior of P(VDF-TrFE) due to the phase transition from ferroelectric to paraelectric in the copolymer. The abrupt increase of losses at low frequencies (<10 kHz) and high temperatures (>65 °C) is a temperature driven process related to increasing ionic conductivity in copolymer, as previously reported. [43–45]

Table1. Dielectric and electromechanical properties of the studied composite and substrate materials.

Material	@ 1 kHz		d_{31} [pm/V]	Y-mod. [GPa]	Pr [$\mu\text{C}/\text{cm}^2$]	Ref.
	ϵ_r	$\tan\delta$				
Pz29	2900	0.019	-240	40 – 60	27.8 ⁶	49
P(VDF-TrFE)	15 ¹	0.03 ¹	8 ¹	1.6 – 1.9 _{2,3}	-	35, 11, 50
PZT-P(VDF-TrFE) with surfactant	58	0.03	-5.1 ⁴ -56 ⁵	1.3	3.36 ⁶	this study
PZT-P(VDF-TrFE) no surfactant	69	0.058	-17 ⁵	1.3	3.76 ⁶	14
Polymer substrate	-	-	-	6	-	this study
Steel foil	-	-	-	195	-	this study

¹P(VDF-TrFE) 56/44 mol%, ²PVDF, ³P(VDF-TrFE) 74/26mol%, ⁴no reinforcement,

⁵steel foil reinforced substrate, ⁶measured at 2.5 Hz and max 28 V/ μm electric field.

The characteristic symmetrical hysteresis behavior for ferroelectric materials is clearly visible in Fig. 5 which shows the polarization in the composite samples as a function of applied voltage. Because of the relatively low permittivity of the polymer matrix compared to the ceramic filler the electric field that was needed to “open” the hysteresis loop was high and the saturation of remanent polarization (P_r) was not reached even with the maximum electric field of 28 V/ μm .

The remanent polarization of samples at about 28 V/ μm was about 3.36 $\mu\text{C}/\text{cm}^2$ (std. dev. $\pm 0.27 \mu\text{C}/\text{cm}^2$) and was about 12 % of a PZ29 ceramic disc's remanent polarization measured with the same parameters at 3 V/ μm . The difference in P_r compared to the earlier ink version without surfactant was about -12 % (3.76 $\mu\text{C}/\text{cm}^2$), which corresponded with the decrease in the permittivity observed in the dielectric measurements. As mentioned earlier, the difference in permittivities of the matrix polymer and ceramic filler and the presence of residual ions generate interface polarizations and space charge polarization in the composites which increases the low frequency permittivity. These also affect the remanent polarization. These polarizations need a relatively high electric field to switch back (or relax) and consequently cause an increase in the measured remanent polarization. Hence, the lower P_r of the surfactant treated ceramic-polymer composite also suggests that the interface or space charge polarizations in the composite have been reduced. [38, 40]

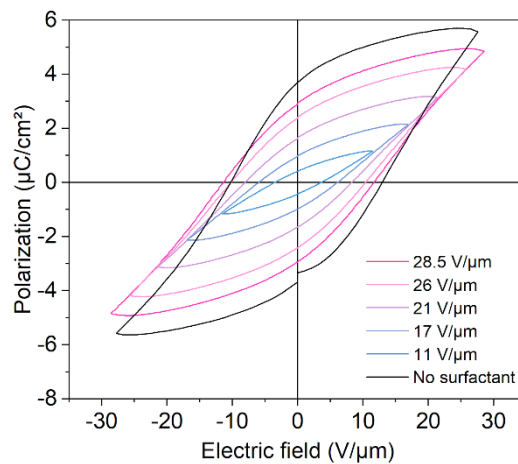


Fig. 5. Polarization in the surfactant treated composite sample in maximum electric fields of 11 V/ μm to 28 V/ μm and in the composite without surfactant treatment in maximum electric field of 28 V/ μm .

Utilizing the converse piezoelectric effect, the effective transverse piezoelectric coefficient $d_{31\text{eff}}$ was defined by measuring the tip displacement of cantilever shaped

samples as a function of voltage. Subsequently, the calculation of the $d_{31\text{eff}}$ was based on the constitutive equations of cantilever benders and measured physical properties: the results are collated in the Table 1. [46, 47] The calculation of both the Young's modulus and $d_{31\text{eff}}$ are provided in the Supplementary Material (Equations S1-S4 and Table S1). Two different substrate configurations were used in the samples: polymer (PET) and steel foil reinforced polymer (PET + steel foil). Fig. 6a shows the displacement of the tip of a cantilever as a function of voltage. Samples were measured at 15 and 60 Hz (well below the resonance frequency of the cantilever). The displacement increased linearly as a function of voltage in both cantilever types (Fig. 6a), which is a characteristic property of the piezoelectric effect (no notable electrostriction). The effect of the stiffer passive layer (steel reinforced polymer substrate) between the sample types was seen as a decreased displacement at the same frequency and voltage and an increased resonance frequency of the cantilever. In Fig. 6b the displacement of the tip of the reinforced type cantilever at 10 Hz is shown in the time domain. The applied voltage polarity was parallel to the poling direction (positive on top) and the displacement was in phase with the applied electric field. This is known behavior of PZT ceramics, which have a negative d_{31} (i.e. an increase in the electric field parallel to the poling polarity results in a decrease in sample length in the transverse direction). Since d_{31} in P(VDF-TrFE) is positive, the result also indicates that the piezoelectric coefficient of ceramic PZ29 particles dominated the effective piezoelectric d_{31} of the composite. [19, 45, 48]

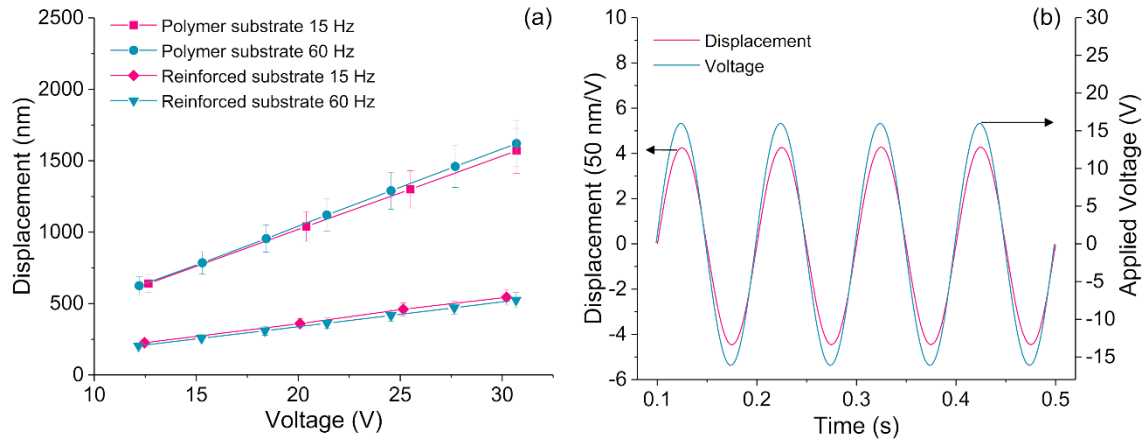


Fig. 6. Typical response from a cantilever sample as a) function of applied voltage (± 10 % variation), b) function of measurement time. In poling, the top electrode was connected to the positive pole of the high voltage source and the bottom electrode to the negative pole. After poling, the positive voltage applied to the top electrode resulted in displacement in the positive direction, i.e. upwards, indicating transversal contraction of the piezoelectric layer.

The $d_{31\text{eff}}$ determined from the polymer substrate cantilevers was small, -5.1 pm/V ($\pm 1 \text{ pm/V}$). This result is consistent with the results reported for 45 vol.% and 51 vol.% by K. W. Kwok et al.. [48] The value of $d_{31\text{eff}}$ was close to the d_{31} of the pure copolymer film, 8 pm/V (Table 1), but with an opposite sign due to the influence of the piezoceramics filler. [11] The small piezoelectric coefficient is reasonable when taking into account that the composite was poled at only in $15 \text{ V}/\mu\text{m}$ to enable comparison with the results from our previous study and that the opposite signed d_{31} coefficients of PZT and P(VDF-TrFE) were partially cancelling each other.

Regardless of the poling conditions the samples with a steel foil reinforced substrate showed an average $d_{31\text{eff}}$ of -56 pm/V (std. dev. $\pm 5 \text{ pm/V}$). This corresponds to as much as 23 % of bulk PZ29 ceramics' d_{31} (-240 pm/V). [49] The difference

between the polymer and the reinforced substrate was huge. The steel layer increased the effective piezoelectric coefficient by ~ 9.8 times. Enhanced electromechanical coupling and maximum energy transmission with stiffer substrate has been reported earlier by Wang et al. [51] in ceramic piezoelectric unimorphs. They have also shown that the blocking force increases with increasing substrates' (or passive layer) Youngs modulus in piezoelectric unimorph structures. [46] However, they have not reported increase in piezoelectric coefficient and the polymer-ceramic composite is mechanically quite different from ceramic materials. Next, two possible causes are suggested for the extraordinary enhancement with steel reinforced substrate

First, cantilever with low Youngs' modulus substrate might suffer from buckling effect in converse piezoelectric measurement. In case of classical buckling rigidity of the structure is suddenly collapsed under critical axial load, with severe deformations and consequences. In contrast to classical case, here the eccentric load is generated for the cantilever by fabrication procedures and piezoelectric layer under actuation. The samples with polymer substrates were significantly curved in the out-of-plane direction after fabrication, thus creating initial internal stresses in the cantilevers. This deformation is likely caused by the shrinkage of the wet ink during curing and the generated internal forces appears to be very close to critical forces in the cantilevers with PET substrate (see example about buckling calculations in Supplementary material). As a consequence of buckling or near buckling situation, the axial rigidity of the cantilevers is decreased, which leads to reduced capability of piezoelectric element to transform its strain into deflection of the tip and lower effective d_{31} coefficient. Calculations of effective d_{31} coefficients assumes linear system where superposition applies [45, 46] and therefore buckling or internal stresses are not regarded which leads here underestimation of the piezoelectric coefficients with PET substrate. However,

when the cantilever is reinforced by steel layer its bending stiffness is greatly increased (~7 times higher critical forces, see Supplementary material) and the sample is also straightened which reduces the internal stresses in the polymer layer. Hence, the axial rigidity in case of steel reinforced samples is sufficient to operate at linear system regime and calculated effective d_{31} coefficients represent actual material properties.

Second proposed reason is that gluing the reinforcement and straightening the cantilever, internal stresses are changed, which may also increase the effective d_{31} .

Previously, it has been discovered that anisotropic and isotropic tensile pre-stress can greatly enhance the effective piezoelectric d_{31} coefficients in pre-stressed actuators [8, 52]. Both or only one of the proposed effects can contribute for significant increase in $d_{31\text{eff}}$. To confirm the theories and for better understanding of the obtained high piezoelectric coefficients, further studies are still needed.

Comparing the measured results to those of the composite without surfactant on the filler particles, the addition of the surfactant treatment increased $d_{31\text{eff}} \sim 3.3$ times. This might not be self-explanatory when taking into account the changes in dielectric and ferroelectric properties. It is suggested that the increase is due to the better mechanical coupling and dispersion of the PZT particles in the copolymer matrix. The coupling is increased as the reactive carboxylic acid anhydride groups of the surfactant are able to bond tightly to the surface of the ceramic particle while the rest of the surfactant molecule bonds with the fluoropolymer matrix, as described earlier by Nelo et al. [53]. Therefore, the mechanical energy is more effectively transferred from polymer to ceramic and vice versa. Similar behavior has been reported with many

silane- based surfactants in 0-3 composites although such improvements in piezoelectric coefficients have not been reported previously [21, 29, 24].

The measured piezoelectric response indicates that with printable piezoelectric composites, the mechanical properties of the matrix and the substrate structure play a very important role when it comes to obtaining the optimum piezoelectric properties for the composite and its usage in components. By improving the structural mechanical coupling (curvature or stiffness of the substrate and filler particle bonding to the matrix), the piezoelectric properties of the PZT may be utilized more effectively.

4. Conclusions

The low temperature cured printable 0-3 ceramic-polymer piezoelectric composite presented here shows one of the highest reported values of $d_{31\text{eff}}$ (-56 pm/V) reported for this type of piezoelectric composite. Surfactant treatment of the piezoceramic filler increased the effective d_{31} coefficient ~3.3 times compared to that of a corresponding sample without surfactant. In addition, a more homogenous distribution of the filler particles and a lack of agglomerates was clearly seen from SEM pictures of the samples' cross-section. The enhanced dispersion and mechanical coupling of the filler and P(VDF-TrFE) matrix together with the prevention of buckling effect by using a stiffer substrate structure are suggested to be responsible for the extraordinarily high converse piezoelectric response of the samples. The high piezoelectric activity and low permittivity and dielectric losses make this ink feasible for actuator and sensor applications. The obtained results also highlight the importance of the composite microstructure and the mechanical structure of the sample or sensor. These should be investigated more thoroughly in future in order to fully utilize them in printable 0-3 piezoelectric composite inks, as has been done in the case of piezoceramics. Through

optimization of e.g. thickness and Young's modulus ratios of different layers, it is likely that an even higher piezoelectric response can be achieved.

Acknowledgements

The authors gratefully acknowledge funding of Academy of Finland (decision n:o 285219) and Tekes (FIMECC program, Hybrid materials project 2105/31/2013). The author TS acknowledges the Tauno Tönning, Walter Ahlström, Emil Aaltonen, KAUTE, Riitta and Jorma J. Takanen and Ulla Tuominen foundations as well as Infotech Oulu Doctoral Program for supporting this study.

Funding

This work was supported by the Academy of Finland (decision n:o 285219) and Tekes (FIMECC program, Hybrid materials project 2105/31/2013).

Appendix A: Supplementary Material

The appendix A includes details of sample structures, calculation of Young's modulus of the composite, the details of the effective d_{31} measurement and calculation, bending curvature results from the two sample types, buckling analysis of the sample cantilevers and cantilever tip displacement vs. electric field measurement.

Data availability statement

The datasets generated during and/or analyzed during the current study are available from the corresponding author on reasonable request.

References

- [1] Z. Cui, *Printed Electronics: Materials, Technologies and Applications*, (Ed: Z. Cui), John Wiley & Sons Singapore Pte. Ltd., Singapore, 2016, p. 1–15.
- [2] S. Khan, L. Lorenzelli, R. S. Dahiya, *IEEE Sens. J.*, 2015, 15, 3164–3185. DOI: <https://doi.org/10.1109/JSEN.2014.2375203>
- [3] T.-C. Huang, K.-T. Chengy, R. Beausoleil, *Printed Circuits on Flexible Substrates: Opportunities and Challenges*, Tenth IEEE/ACM International Symposium on Networks-on-Chip (NOCS), 2015, 1,1–4. <https://doi.org/10.1109/NOCS.2016.7579340>
- [4] J. Zhou, T. Ge, E. Ng, J. S. Chang, *IEEE T. Electron. Dev.*, 2016, 63, 793–799. <https://doi.org/10.1109/TED.2015.2508484>
- [5] Y. Lin, H. A. Sodano, *Adv. Funct. Mater.*, 2009, 19, 592–598. <https://doi.org/10.1002/adfm.200800859>
- [6] S. Gebhardt, L. Seffner, F. Schlenkrich, A. Schönecker, *J. Eur. Ceram. Soc.*, 2007, 27, 4177–4180. <https://doi.org/10.1016/j.jeurceramsoc.2007.02.122>
- [7] J. Juuti, K. Kordás, R. Lonnakko, V.-P. Moilanen, S. Leppävuori, *Sensor. Actuator A-Phys.* 2005, 120, 225–231. <https://doi.org/10.1016/j.sna.2004.11.016>
- [8] J. Juuti, H. Jantunen, V.-P. Moilanen, S. Leppävuori, *IEEE T. Ultrason. Ferr.*, 2006, 53, 838-846.
- [9] M. Leinonen, J. Juuti, H. Jantunen, J. Palosaari, *Energy Technol.*, 2016, 4, 620–624. <https://doi.org/10.1002/ente.201500429>
- [10] H. Li, C. Tian, Z. D. Deng, *Appl. Phys. Reviews*, 2014, 1, 041301-1–20. <https://doi.org/10.1063/1.4900845>
- [11] K. Koga, H. Ohigashi, *J. Appl. Phys.*, 1986), 59, 2142–2150. <https://doi.org/10.1063/1.336351>

- [12] T. Yagi, M. Tatemoto, J.-I. Sako, *Polym. J.*, 1980, 12, 209–223.
- [13] J.-H. Lee, H.-J. Yoon, T. Y. Kim, M. K. Gupta, J. H. Lee, W. Seung, H. Ryu, S.-W. Kim, *Adv. Funct. Mater.*, 2015, 25, 3202–3209.
<https://doi.org/10.1002/adfm.201500856>
- [14] T. Siponkoski, M. Nelo, J. Palosaari, J. Peräntie, M. Sobocinski, J. Juuti, H. Jantunen, *Compos. Pt. B-Eng.*, 2015, 80, 217–222.
<https://doi.org/10.1016/j.compositesb.2015.05.018>
- [15] T. Siponkoski, M. Nelo, J. Peräntie, J. Juuti, H. Jantunen, *Compos. Pt. B-Eng.*, 2015, 70, 201–205. <https://doi.org/10.1016/j.compositesb.2014.11.017>
- [16] X. X. Wang, K. H. Lam, X. G. Tang, H. L. W. Chan, *Solid State Commun.*, 2004, 130, 695–699. <https://doi.org/10.1016/j.ssc.2004.03.020>
- [17] H.-G. Lee, H.-G. Kim, *J. Appl. Phys.*, 1990, 67, 2024–2028.
<https://doi.org/10.1063/1.345584>
- [18] H. L. W. Chan, Y. Chen, C. L. Choy, *IEEE T. Dielect. El. In.* 1996, 3, 800–805.
- [19] H. L. W. Chan, P. K. L. Ng, C. L. Choy, *Appl. Phys. Lett.*, 1999, 74, 3029–3031.
<https://doi.org/10.1063/1.124054>
- [20] T. Vuorinen, M. Zakrzewski, S. Rajala, D. Lupo, J. Vanhala, K. Palovuori, S. Tuukkanen, *Adv. Funct. Mater.*, 2014, 24, 6340–6347.
<https://doi.org/10.1002/adfm.201401140>
- [21] T. Zhou, J.-W. Zha, R.-Y. Cui, B.-H. Fan, J.-K. Yuan, Z.-M. Dang, *ACS Appl. Mater. Interfaces*, 2011, 3, 2184–2188. <https://doi.org/10.1021/am200492q>
- [22] Y. Song, Y. Shen, H. Liu, Y. Lin, M. Li, C.-W. Nan, *J. Mater. Chem.*, 2012, 22, 8063–8068. <https://doi.org/10.1039/c2jm30297g>
- [23] S. Cho, J. S. Lee, J. Jang, *Adv. Mater. Interfaces*, 2015, 2, 1500098-1–13.
<https://doi.org/10.1002/admi.201500098>

- [24] D.I. Tee, M. Mariatti, A. Azizan, C. H. See, K. F. Chong, *Compos. Sci. Technol.*, 2007, 67, 2584–2591. <https://doi.org/10.1016/j.compscitech.2006.12.007>
- [25] W. Xu, H.-L. Huang, Y. Liu, C. Luo, G. Z. Cao, I. Y. Shen, *Sensor. Actuator A-Phys.*, 2016, 246, 102–113. <https://doi.org/10.1016/j.sna.2016.05.010>
- [26] X. Zhang, Y. Ma, C. Zhao, W. Yang, *Appl. Surf. Sci.*, 2014, 305, 531–538. <https://doi.org/10.1016/j.apsusc.2014.03.131>
- [27] Q. Zhang, F. Gao, C. Zhang, L. Wang, M. Wang, M. Qin, G. Hu, J. Kong, *Compos. Sci. Technol.*, 2016, 129, 93–100. <https://doi.org/10.1016/j.compscitech.2016.04.016>
- [28] L. Ramajo, M. S. Castro, M. M. Reboredo, *Compos. Pt. A-Phys.*, 2007, 38, 1852–1859. <https://doi.org/10.1016/j.compositesa.2007.04.003>
- [29] K. Kim, J. L. Middlebrook, J. E. Chen, W. Zhu, S. Chen, D. J. Sirbuly, *ACS Appl. Mater. Interfaces*, 2016, 8, 33394–33398. <https://doi.org/10.1021/acsami.6b12086>
- [30] J. L. Lutkenhaus, K. McEnnis, A. Serghei, T. P. Russell, *Macromolecules*, 2010, 43, 3844–3850. <https://doi.org/10.1021/ma100166a>
- [31] S. S. Guo, X. H. Sun, S. X. Wang, S. Xu, X.-Z. Zhao, H. L.W. Chan, *Mater. Chem. Phys.*, 2005, 91, 348–354. <https://doi.org/10.1016/j.matchemphys.2004.11.038>
- [32] V. S. Nguyen, D. Rouxel, M. Meier, B. Vincent, A. Dahoun, S. Thomas, F. D. Dos Santos, *Polym. Eng. Sci.*, 2014, 54, 1280–1288. <https://doi.org/10.1002/pen.23670>
- [33] H. N. da Cunha, L. H. C. Mattoso, R. M. Faria, *J. Polym. Sci. Pol. Phys.*, 1996, 35, 1201–1205. [https://doi.org/10.1002/\(SICI\)1099-0488\(199706\)35:8<1201::AID-POLB5>3.0.CO;2-W](https://doi.org/10.1002/(SICI)1099-0488(199706)35:8<1201::AID-POLB5>3.0.CO;2-W)

- [34] B. Ploss, B. Ploss, *Polymer*, 2000, 41, 6087-6093. [https://doi.org/10.1016/S0032-3861\(99\)00861-7](https://doi.org/10.1016/S0032-3861(99)00861-7)
- [35] G. Perrier, A. Bergeret, *J. Polym. Sci. B Polym. Phys.*, 1997, 35, 1349-1359. [https://doi.org/10.1002/\(SICI\)1099-0488\(19970715\)35:9<1349::AID-POLB5>3.0.CO;2-H](https://doi.org/10.1002/(SICI)1099-0488(19970715)35:9<1349::AID-POLB5>3.0.CO;2-H)
- [36] M. Arous, A. Kallel, Z. Fakhfakh, G. Perrier, *Composite Interfaces*, 1997, 5, 137-153, <https://doi.org/10.1163/156855497X00118>
- [37] Y. Song, Y. Shen, H. Liu, Y. Lin, M. Li, C.-W. Nan, *J. Mater. Chem.*, 2012, 22, 16491-16498. <https://doi.org/10.1039/c2jm32579a>
- [38] K. Yu, Y. Niu, Y. Bai, Y. Zhou, H. Wang, *Appl. Phys. Lett.*, 2013, 102, 102903-1-5. <https://doi.org/10.1063/1.4795017>
- [39] T. Zhou, J.-W. Zha, R.-Y. Cui, B.-H. Fan, J.-K. Yuan, Z.-M. Dang, *ACS Appl. Mater. Interfaces*, 2011, 3, 2184-2188. <https://doi.org/10.1021/am200492q>
- [40] S. Cho, J. S. Lee, J. Jang, *Adv. Mater. Interfaces*, 2015, 2, 1500098-1-13. <https://doi.org/10.1002/admi.201500098>
- [41] X. Zhang, Y. Ma, C. Zhao, W. Yang, *Appl. Surf. Sci.*, 2014, 305, 531-538. <https://doi.org/10.1016/j.apsusc.2014.03.131>
- [42] T. Yagi, M. Tatemoto, J.I. Sako, *Polym. J.*, 1980, 12, 209-223. <https://doi.org/10.1295/polymj.12.209>
- [43] Y. Tajitsu, A. Chiba, T. Furukawa, M. Date, E. Fukada, *Appl. Phys. Lett.*, 1980, 36, 286-288. <https://doi.org/10.1063/1.91456>
- [44] M. Dietze, J. Krause, C.-H. Solterbeck, M. Es-Souni, *J. Appl. Phys.*, 2007, 101, 054113-1-7. <https://doi.org/10.1063/1.2653978>
- [45] J. G. Smits, W.-S. Choi, *IEEE T. Ultrason. Ferr.*, 1991, 38, 256-270. <https://doi.org/10.1109/ULTSYM.1990.171567>

- [46] Q.-M. Wang, L. E. Cross, *Ferroelectrics*, 1998, 215, 187-213.
<https://doi.org/10.1080/00150199808229562>
- [47] R. Zeng, K. W. Kwok, H. L. W. Chan, C. L. Choy, *J. Appl. Phys.*, 2002, 92, 2674-2679. <https://doi.org/10.1063/1.1497699>
- [48] MSSDK_PZ29_Datasheet-201711, PZ29 Datasheet, Meggitt A/S,
<https://www.meggittferroperm.com> (accessed 21 September 2018)
- [49] P. Thongsanitgarn, A. Watcharapasorn, S. Jiansirisomboon, *Surf. Rev. Lett.*, 2010, 17, 1-7. <https://doi.org/10.1142/S0218625X10013540>
- [50] A. Almusallam, Z. Luo, A. Komolafe, K. Yang, A. Robinson, R. Torah, S. Beeby, *Nano Energy*, 2017, 33, 146-156. <https://doi.org/10.1016/j.nanoen.2017.01.037>
- [51] Q.-M. Wang, X.-H. Du, B. Xu, L. E. Cross, *IEEE Trans Ultrason. Ferroelectr. Freq. Control*, 1999, 46, 638-646. <https://doi.org/10.1109/58.764850>
- [52] R. W. Schwartz, L. E. Cross, Q.-M. Wang, *J. Amer. Ceram. Soc.*, 2001, 84, 2563-2569. <https://doi.org/10.1111/j.1151-2916.2001.tb01054.x>
- [53] M. Nelo, A. K. Sowpati, V. K. Palukuru, J. Juuti, H. Jantunen, *Prog. Electromagn. Res.*, 2010, 110, 253-266.